

PM3 study of the domino reaction of nitroalkenes with silyl enol ethers

Luis R. Domingo,^{1*} M. Teresa Picher¹ and Juan Andrés²

¹Departamento de Química Orgánica, Universidad de Valencia, Dr Moliner 50, 46100 Burjassot, Valencia, Spain

²Departament de Ciències Experimentals, Universitat Jaume I, Apartat 224, 12080 Castelló, Spain

Received 30 October 1997; revised 15 February 1998; accepted 27 April 1998

ABSTRACT: The molecular mechanism of the domino reaction of nitroalkenes with silyl enol ethers to give nitroso acetal adducts was characterized using computational procedures at the PM3 semiempirical level. The domino process comprises three consecutive steps: the first and rate-determining step is the nucleophilic attack of the silyl enol ether on the nitroalkene to give a zwitterionic intermediate; closure of this intermediate leads to a nitronate intermediate, which then affords the final nitroso acetal adduct through an intramolecular [3 + 2] cycloaddition. The presence of both silicon and oxygen atoms in the silyl enol ether increases the nucleophilic character of the carbon–carbon double bond and favors the ionic character of the first step. The presence of the Lewis acid promotes the delocalization of the negative charge transferred in the nucleophilic attack of the silyl enol ether to the nitroalkene and decreases the activation energy of the rate-determining step. The inclusion of solvent effects predicts a stabilization of the first zwitterionic intermediate and therefore emphasizes the stepwise mechanism for the first cycloaddition of this domino reaction. Copyright © 1999 John Wiley & Sons, Ltd.

KEYWORDS: nitroalkenes; silyl enol ethers; domino reaction; PM3 semiempirical method

INTRODUCTION

Domino cycloadditions play a key role in organic syntheses where construction of complex polycyclic structures with adequate regio- and stereochemical control is needed.^{1–3} In this type of process, several bonds of the target molecule are formed alongside a continuous sequence of reactions which do not require isolation of intermediates, changes of reaction conditions or addition of reagents. The interest in the subject is shown by numerous recent reviews.^{2–7}

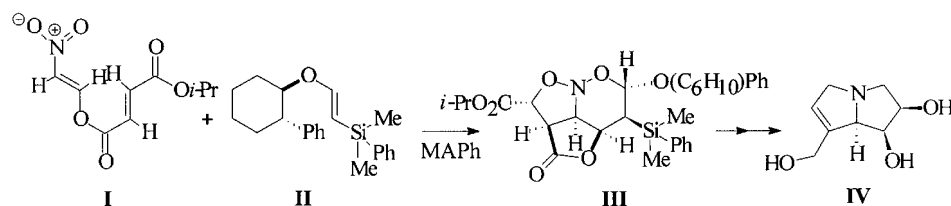
Among domino-type reactions, those involving nitroalkenes have been extensively developed for the stereoselective construction of polycyclic nitrogen-containing compounds.⁴ Denmark and Thorarensen⁸ recently described the domino reaction of the nitroalkene **I** with the silyl enol ether **II** in the presence of the Lewis acid MAPH to give the nitrosoacetal **III**, an intermediate in the synthesis of (+)-crotanecine (**IV**) (Scheme 1). In their view, the process consists of two consecutive [4 + 2] intermolecular/[3 + 2] intramolecular cycloadditions, the first one having a stepwise mechanism.⁸ The stepwise

mechanism was proposed on the basis of previous experimental work⁹ on [4 + 2] cycloadditions of nitroalkenes with simple acyclic and cyclic alkenes in the presence of SnCl₄. The formation of cyclic five-membered side-products was only accountable through a Wagner–Meerwein shift in a zwitterionic intermediate. However, no similar rearrangements products were found in the domino reactions involving silyl enol ethers.⁸ This shows that the mechanism of this type of domino reaction may be profoundly influenced by variations in the electronic features of either the alkene and the Lewis acid.

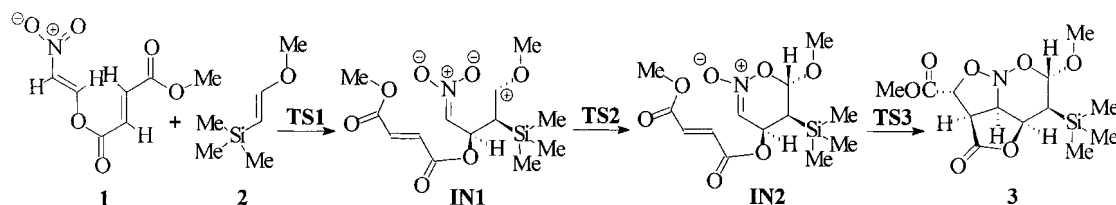
Despite the obvious potential of the domino process and its many variations, the reaction pathway has not yet been studied theoretically. A deep knowledge of the molecular mechanism is fundamental, however, for a rationalization of the experimental results. We are engaged at present in a research program involving the computational study of domino cycloaddition reactions.¹⁰ In this work, we studied the reaction of the nitroalkene **1** with the silyl enol ether **2** to yield the nitroso acetal adduct **3** (Scheme 2) at the PM3 semiempirical level. The effect of both Lewis acid and solvents was included in the study. Our purpose is to contribute to a better mechanistic understanding of this type of domino process, especially by characterization of the stationary points on the reactive potential energy surface (PES).

*Correspondence to: L. R. Domingo, Departamento de Química Orgánica, Universidad de Valencia, Dr Moliner 50, 46100 Burjassot, Valencia, Spain.

Contract/grant sponsor: Conselleria de Cultura Educació i Ciència, Generalitat Valenciana; Contract/grant number: GV97-CB11-96.



Scheme 1



Scheme 2. Schematic representation of the stepwise mechanism of the domino reaction between the nitroalkene **1** and the silyl enol ether **2**

COMPUTATIONAL METHODS AND MODELS

Semiempirical restricted Hartree–Fock calculations were carried out with the MOPAC93 package of programs¹¹ using the PM3 method.¹² The PES was calculated in detail to ensure that all relevant stationary points were located and properly characterized. The optimizations were carried out using the eigenvalue following routine,¹³ and the requested convergence for the gradients of energy was 0.5 kcal mol⁻¹ Å rad⁻¹ (1 kcal = 4.184 kJ). The nature of each stationary point was checked by diagonalization of the Hessian matrix in order to determine the number of imaginary frequencies (zero for local minima and one for transition structure).

Geometry optimizations of the stationary structures including the Lewis acid and the solvent effects were carried out at the PM3 semiempirical level using the conductor-like screening model (COSMO) option,¹⁴ included in the MOPAC93 package program. This COSMO model, proposed by Klamt and Schüürmann,¹⁴ calculates the electrostatic solvation energy by representing the solute charge distribution as a set of point charges and dipoles in the neglect differential diatomic overlap formalism. In this procedure, the solvent is assimilated to a continuous medium characterized by its dielectric constant (ϵ), which surrounds a molecular-shaped cavity in which the solute is placed. The solvent used in the experimental work was toluene.⁸ Therefore, we used the dielectric constant at 296.4 K, $\epsilon = 2.38$. In spite of the low solvent dielectric constant, it is possible to make qualitative observations regarding the stabilization of ionic species which appear in the different reaction pathways.

We used the simplified models **1** and **2** instead of nitroalkene **I** and silyl enol ether **II**, respectively. In Denmark and Thorarensen's nitroalkene **I** the isopropyl

group was replaced by a methyl group. In silyl enol ether **II**, the Si-bonded phenyl residue was replaced by a methyl group. Furthermore, the bulky chiral cyclohexyl appendage was replaced by a non-chiral methyl group. The role of the acidic catalyst in the molecular mechanism was studied using AlMe₃ as a Lewis acid model. Since the large steric demand of the bulky Lewis acid used in the experimental work allows only the *exo* mode attack,¹⁵ we have considered exclusively this *exo* mode in the present study.

RESULTS AND DISCUSSION

Gas-phase calculations

The energy profile showing the position of stationary points along the reaction pathway is depicted in Fig. 1 and PM3 heats of formation of these stationary points are presented in Table 1, pathway a. One intermediate, **IN2**, and three TSs, **TS1**, **TS2** and **TS3**, were located on the PES in the gas-phase reaction pathway of the non-catalyzed process.

The analysis of the gas-phase energies shows that this domino reaction is an exothermic process (−22.5 kcal mol⁻¹) and that the first step is rate determining (the activation energy of the first step is 31.8 kcal mol⁻¹). The geometries of the transition structures are depicted in Fig. 2. **TS1** corresponds to a nucleophilic attack of C-6 in the silyl enol ether on C-5 in the nitroalkene. The length of the C-5—C-6 bond being formed in **TS1** is 1.776 Å, while the O-1—C-7 distance (2.771 Å) shows that these atoms are not bonded. All attempts to find the intermediate **IN1** as a minimum were unsuccessful, as in the gas phase the PES in this region is very flat (for **TS2** the imaginary frequency is 50i cm⁻¹).

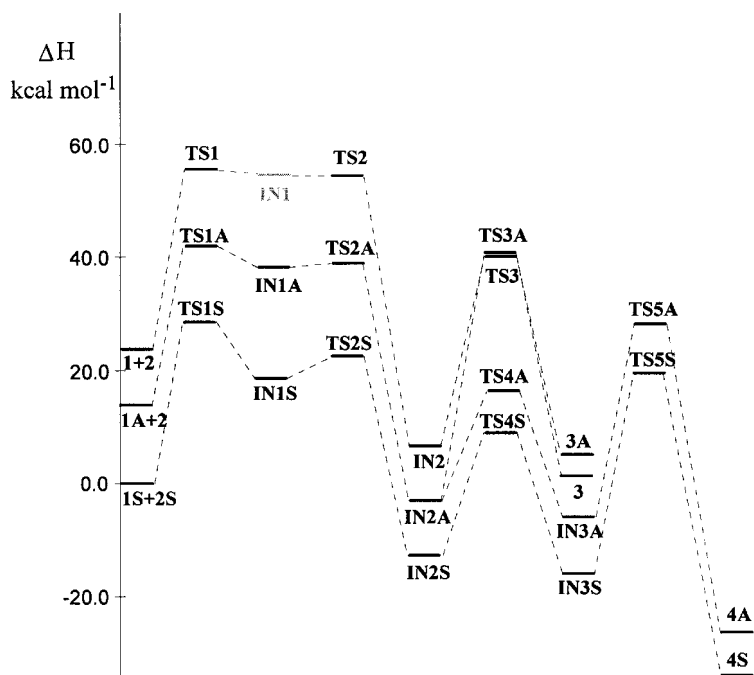


Figure 1. Schematic representation of the energy profiles for the domino reaction between the nitroalkene **1** and the silyl enol ether **2**. Profile A corresponds to the AlMe_3 -catalyzed process and profile S to the catalyzed reaction in toluene solvent

Table 1. PM3 heats of formation, ΔH°_f , (kcal mol^{-1}), for the stationary points of the domino reaction between the nitroalkene **1** and the silyl enol ether **2**

Pathway ^a	1	2	TS1	IN1	TS2	IN2	TS3	3	TS4	IN3	TS5	4
a	-133.7	-69.9	-171.8		-173.2	-221.0	-187.8	-226.1				
b	-149.6	-69.9	-191.5	-195.1	-194.6	-236.6	-192.5	-228.0	-216.0	-237.7	-204.5	-258.4
c	-162.5	-71.5	-204.7	-214.7	-210.8	-246.0	-200.4	-235.2	-223.4	-248.1	-212.6	-265.9

^a a, Non-catalyzed pathway; b, catalyzed pathway (AlMe_3 , $\Delta H^\circ_f = -5.72 \text{ kcal mol}^{-1}$); c, catalyzed pathway in toluene solvent.

These facts indicate that the **IN1** and **TS2** stationary points are structurally and energetically related. **TS2** corresponds to the closure of **IN1** by means of nucleophilic attack of the O-1 atom on the carbocationic C-7 center, giving **IN2**. The length of the O-1—C-7 bond being formed in **TS2** is 2.609 Å. Finally, **TS3** corresponds to a synchronous concerted [3 + 2] cycloaddition. The lengths of the O-3—C-11 and C-4—C-10 bonds being formed in **TS3** are 2.077 and 2.047 Å, respectively. The nucleophilic attack of C-6 on the C-5 center in the first step is responsible for the high regioselectivity observed experimentally.

The C-7—O-8 bond length in **TS1** (1.320 Å) is smaller than that in silyl enol ether **2** (1.382 Å), and becomes even shorter in **TS2** (1.311 Å), finally increasing in intermediate **IN2** (1.438 Å). The C-6—C-7—O-8 bond angle in **TS1** and **TS2** is *ca* 118°, in agreement with sp^2 hybridization for the C-7 atom, whereas in intermediate **IN2** this angle becomes 107°, corresponding to sp^3 hybridization. Finally, the C-6—C-7—O-8—C-9 dihedral angle in **TS1** and **TS2** is *ca* 176°, whereas for

intermediate **IN2** it is 247°. These geometric parameters, together with the increment of positive charge at the C-7 atom on going from **2** (0.0 u.a.) to **TS1** and **TS2** (0.3 u.a.), indicate the formation of a carbocationic center at C-7 in **TS1**, stabilized by the delocalization of the lone pair of the oxygen atom O-8. Moreover, the electron-releasing character of the silicon atom renders the silyl enol ether a powerful nucleophile, whereby a larger negative charge is developed at C-6. In fact, for a hypothetical system formally derived from **2** by replacing the silicon by a carbon atom, PM3 calculations yield an activation energy of $38.1 \text{ kcal mol}^{-1}$ for the first step ($6.3 \text{ kcal mol}^{-1}$ higher than for **TS1**).

Study of the role of the Lewis acid

It has been assumed that the Lewis acid is coordinated to an oxygen atom of the nitro group.⁸ We therefore reoptimized the stationary points with inclusion of AlMe_3 as a Lewis acidic catalyst. Figure 1 shows the location of

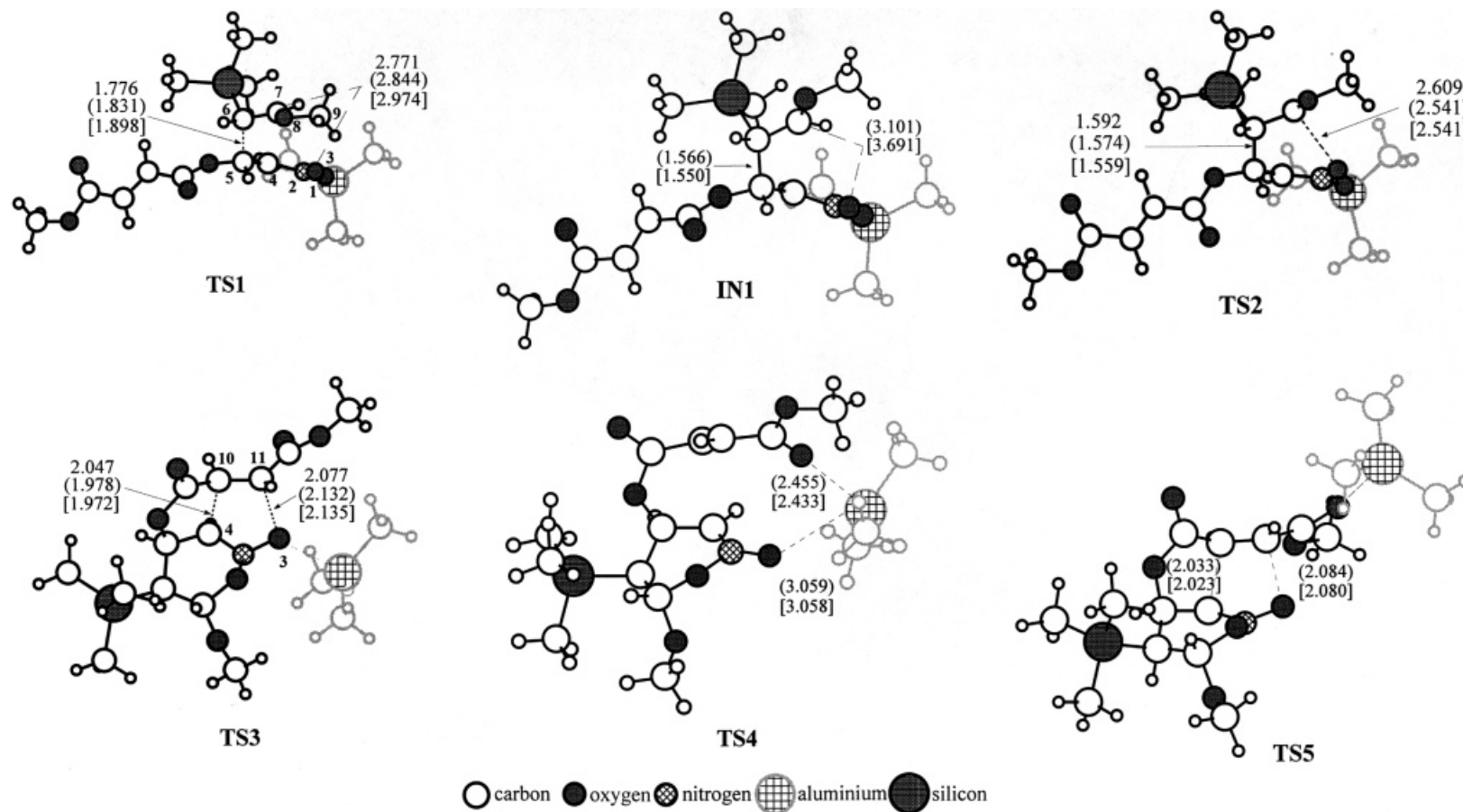
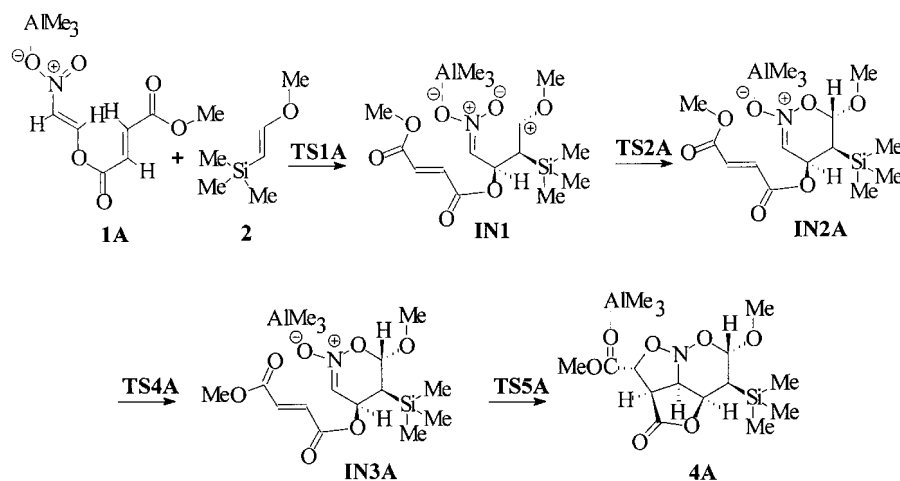


Figure 2. PM3 transition structures corresponding to the domino reaction between the nitroalkene **1** and the silyl enol ether **2**. The values of the bond lengths directly involved in the processes are given in Ångströms. The values in parentheses correspond to the catalyzed reaction and the values in square brackets correspond to the catalyzed reaction in toluene solvent. Relative positions of AlMe_3 are depicted



Scheme 3. Schematic representation of the catalyzed mechanism of the domino reaction between the nitroalkene **1** and the silyl enol ether **2**

the stationary points along the catalyzed reaction pathway, while the selected geometrical parameters for TSs are given in Fig. 2. Scheme 3 shows reactants, **1A** and **2**, intermediates, **IN1A**, **IN2A** and **IN3A**, and product, **4A**, with the catalyzed process. The energy results are given in Table 1, pathway b.

The presence of the Lewis acid decreases the activation energy for the first and rate-determining step owing to delocalization of the charge transferred to the nitroalkene system. This stabilization allows one to find the intermediate **IN1A** as a minimum on the reactive PES. The C-5—C-6 bond length in **IN1A** is 1.566 Å, whereas the distance between the O-1 and C-7 atoms is 3.101 Å. This distance, which is longer than in **TS1A** (2.844 Å), indicates that these atoms are not bonded in this intermediate. In the intramolecular [3 + 2] cycloaddition, the presence of the Lewis acid causes an opposite effect, as it increases the activation energy of the third step. Thus, **TS3A** and the adduct **3A** are the more destabilized species, intermediate **IN2A** being more stable than the final adduct **3A** (see Fig. 1).

Coordination of the Lewis acid to O-3 in the nitronate group of **IN2** makes the third step an endothermic process (8.6 kcal mol⁻¹). However, a detailed exploration of PES allows one to find an alternative channel associated with the change of Lewis acid coordination from the oxygen atom of the nitronate group to an oxygen atom of the carboxyl group on C-11, via the transition structure **TS4A** (the activation energy associated with **TS4A** is 20.6 kcal mol⁻¹). This process allows an equilibration between intermediates **IN2A** and **IN3A**, with **IN3A** being 1.1 kcal mol⁻¹ more stable than **IN2A**.

Finally, the intramolecular [3 + 2] cycloaddition of intermediate **IN3A**, via the transition structure **TS5A**, affords the more stable cycloadduct **4A**. The activation energy associated with **TS5A** (33.2 kcal mol⁻¹) is lower than that for **TS3A** (44.1 kcal mol⁻¹), this cycloaddition being an exothermic process (−20.7 kcal mol⁻¹). The transi-

tion structure **TS5A** corresponds to a synchronous concerted process where the lengths of the O-3—C-11 and C-4—C-10 bonds being formed are 2.084 and 2.033 Å, respectively.

The analysis of the molecular orbitals of **TS1** and **TS1A** indicates a large stabilization of the HOMO involved in this process for **TS1A** relative to **TS1** (−8.81 and −8.30 eV, respectively). This can be understood as a stronger HOMO delocalization in **TS1A** due to the participation of the aluminum atom.

The step connecting the intermediate **IN2** with the adduct **3** is disfavored by the presence of AlMe_3 , and the activation energy associated with **TS3A** increases by 10.9 kcal mol⁻¹ with respect to **TS3**. This can be also explained by means of an analysis of molecular orbitals. In the third step, which corresponds to an intramolecular [3 + 2] cycloaddition with normal electron demand, the AlMe_3 located in the donor dipole fragment does not contribute to the negative charge transfer to the acceptor dipolarophile fragment. In consequence, an increase in the energy of the HOMO at **TS3A** (the increments of energies of the HOMOs for the non-catalyzed and catalyzed processes are 0.43 and 0.69 eV, respectively) is observed. However, when the AlMe_3 is located at the acceptor fragment (interaction with the carboxyl group at C-11), the increment of the HOMO energy at **TS5A** is lower than that at **TS3** (0.30 eV). This shows that the Lewis acid stabilizes this MO slightly. Both **TS3** and **TS5A** have very similar activation energies (around 33.2 kcal mol⁻¹).

A comparison of the geometric parameters of these stationary points with those of the non-catalyzed mechanism shows marginal differences in the geometries of the stationary points. For **TS1A**, the length of the C-5—C-6 bond being formed is 1.831 Å, which is slightly longer than that for **TS1**. For **TS2A**, the O-1—C-7 distance decreases from 2.609 to 2.541 Å on going from the non-catalyzed to the catalyzed reaction. **TS3A** for the

intramolecular [3 + 2] cycloaddition is slightly more asynchronous than for the non-catalyzed reaction, the lengths of the O-3—C-11 and C-4—C-10 bonds being formed being 2.132 and 1.978 Å, respectively. Finally, the comparison of these bond lengths between **TS3** and **TS5A** (see Fig. 2) shows very close values, in agreement with the similar activation energies found for these transition structures.

Study of the solvent effect

Solvent effects on [4 + 2] cycloaddition are well known¹⁶ and have received considerable attention, especially in the last few years.^{17–19} A pictorial representation of the PES in toluene, including the position of the stationary points, is depicted in Fig. 1, and the selected geometric parameters of the stationary points with inclusion of the solvent effects are given in Fig. 2. An analysis of these results indicates that there are not large modifications in the geometry for these stationary points. This agrees well with the hypothesis of Tomasi and co-workers²⁰ that, in the case of minima, the approximation of frozen geometries can often be considered adequate. Although this can be more questionable in the case of TSs, only small modifications of the geometry of TSs in solution are detected.¹⁹

Table 1, pathway c, gives the PM3 heats of formation of the optimized stationary points with inclusion of solvent effects. The solvent effects cause a larger stabilization for nitroalkene **1S** (–12.9 kcal mol^{–1}) than for silyl enol ether **2S** (–1.6 kcal mol^{–1}) owing to the presence of the Lewis acid coordinated to the polar nitroalkene group. This stabilization is also present in **TS1S**, **IN1S**, **TS2S** and **IN2S**. The intermediate **IN1S** is more stabilized (–19.6 kcal mol^{–1}) than **TS1S** and **TS2S** (–13.2 and –16.1 kcal mol^{–1}), owing to the large polar character of this zwitterionic intermediate. Hence the solvent appears to stimulate a stepwise mechanism for the first cycloaddition.¹⁹ These results are related to the larger charge transfer in the electrophilic attack in the first step of the intermolecular cycloaddition, as shown by the large increment of the dipole moments along this pathway (dipole moments for **1A**, **2**, **TS1A**, **IN1A**, **TS2A** and **IN2A** are 7.73, 1.55, 10.24, 14.16, 12.99 and 6.34 D, respectively).

The solvent effects cause a minor stabilization for the remaining stationary points of this domino reaction (between 7.2 and 10.4 kcal mol^{–1}), due to the minor polar character of these species. Hence the main factor resulting from inclusion of solvent effects is the large stabilization of the intermediate **IN1S**, making the nucleophilic attack of the silyl enol ether to the nitroalkene essentially irreversible.

CONCLUSIONS

We have carried out a theoretical study of the domino reaction between nitroalkenes and silyl enol ethers. Reaction pathways in the presence and absence of AlMe₃ as a model Lewis acidic catalyst were studied using PM3 semiempirical methods with inclusion of solvent effects. Specific details of the overall process may change at higher levels of theory (e.g. *ab initio* methods with inclusion of correlation energy) but, despite the approximate nature of the calculations employed here, some important features have been clarified. The following conclusions can be drawn from the results obtained in this study: (1) the overall process comprises a three-step mechanism; (2) the first and rate-determining step is the nucleophilic attack of the silyl enol ether on the nitroalkene to give a zwitterionic intermediate; the second step corresponds to a ring closure of this intermediate to give a cyclic nitronate which leads in the third step, through an intramolecular [3 + 2] cycloaddition, to the nitroso acetal adduct; (3) the nucleophilic character of the first step is responsible for the high regioselectivity observed in this reaction; (4) the presence of both silicon and oxygen atoms in the silyl enol ether increases the nucleophilic character of the carbon–carbon double bond and therefore favors the ionic character of the first step; (5) the coordination of a Lewis acid to an oxygen atom of the nitro group decreases the activation energy for the initial nucleophilic attack, owing to a larger delocalization of the negative charge transferred from the nucleophile fragment to the nitroalkene system; and (6) the inclusion of the solvent effects makes the electrophilic attack of the silyl enol ether on the nitroalkene an irreversible process, owing to the large stabilization of the zwitterionic intermediate formed.

Acknowledgments

This work was supported by research funds provided by the Conselleria de Cultura Educació i Ciència, Generalitat Valenciana (Project GV97-CB11-96). The authors thank Professors R. Mestres and J. A. Marco for helpful comments. All calculations were performed on a IBM POWER PC-250 workstation at the Departamento de Química Orgánica of the Universidad de Valencia.

REFERENCES

1. L. F. Tietze. *Chem. Rev.* **96**, 115 (1996).
2. (a) L. F. Tietze. *Chem. Ind. (London)* 453 (1995); (b) L. F. Tietze and U. Beifuss. *Angew. Chem., Int Ed. Engl.* **32**, 131 (1993); (c) L. F. Tietze, J. Bachmann, J. Wichmann and O. Burkhard. *Synthesis* 1185 (1994).
3. W. Carruthers. *Cycloaddition Reactions in Organic Synthesis*, Chapt. 1–3. Pergamon Press, Oxford (1990).

4. S. E. Denmark and A. Thorarensen. *Chem. Rev.* **96**, 137 (1996).
5. J. D. Winkler. *Chem. Rev.* **96**, 167 (1996).
6. (a) R. A. Bunce. *Tetrahedron* **51**, 13103 (1995); (b) I. Ryu, N. Sonoda and D. P. Curran. *Chem. Rev.* **96**, 177 (1996); (c) P. J. Parson, C. S. Penkett and A. J. Shell. *Chem. Rev.* **96**, 195 (1996); (d) K. K. Wang. *Chem. Rev.* **96**, 207 (1996); (e) A. Padwa and M. D. Weingarten. *Chem. Rev.* **96**, 223 (1996).
7. (a) T. L. Ho. *Tandem Organic Reactions*. Wiley, New York, (1992); (b) C. Thebtaranonth and Y. Thebtaranonth. *Cyclization Reactions*. CRC Press, Boca Raton, FL (1994).
8. S. E. Denmark and A. Thorarensen. *J. Am. Chem. Soc.* **119**, 125 (1997).
9. (a) S. E. Denmark, Y.-C. Moon, C. J. Cramer, M. S. Dappem and C. B. W. Senanayake. *Tetrahedron* **46**, 7373 (1990); (b) S. E. Denmark, C. J. Cramer and J. A. Sternberg. *Helv. Chim. Acta* **69**, 1871 (1986).
10. (a) L. R. Domingo, M. Arnó and J. Andrés. *Tetrahedron Lett.* **37**, 7573 (1996); (b) L. R. Domingo, M. Arnó and J. Andrés. *J. Am. Chem. Soc.* **120**, 1618 (1998); (c) L. R. Domingo, M. T. Picher, M. Arnó, J. Andrés and V. S. Safont. *J. Mol. Struct. (Theochem)* **426**, 257 (1998).
11. J. J. P. Stewart. *MOPAC 93*. Fujitsu, Tokyo (1993).
12. J. J. P. Stewart. *J. Comput. Chem.* **10**, 209 (1989).
13. J. Baker. *J. Comput. Chem.* **7**, 385 (1986).
14. A. Klamt and G. Shüürmann. *J. Chem. Soc., Perkin Trans. 2* 799 (1993).
15. S. E. Denmark, M. E. Schnute, L. R. Marcin and A. Thorarensen. *J. Am. Chem. Soc.* **60**, 3205 (1995).
16. (a) U. Pindur, G. Lutz and C. Otto. *Chem. Rev.* **93**, 741 (1993); (b) C. -J. Li. *Chem. Rev.* **93**, 2023 (1993); (c) W. Blokzijl and J. B. F. N. Engberts. *Angew. Chem., Int. Ed. Engl.* **32**, 1545 (1993).
17. (a) J. F. Blake and W. L. Jorgensen. *J. Am. Chem. Soc.* **113**, 7430 (1991); (b) M. F. Ruiz-López, X. Assfeld, J. I. García, J. A. Mayoral and L. Salvatella. *J. Am. Chem. Soc.* **115**, 8780 (1993); (c) C. Cativiela, V. Dillet, J. I. García, J. A. Mayoral, M. F. Ruiz-López and L. Salvatella. *J. Mol. Struct. (Theochem)* **331**, 37 (1995).
18. (a) W. L. Jorgensen, D. Lim, J. F. Blake and D. L. Severance. *J. Chem. Soc., Faraday Trans.* **90**, 1727 (1994); (b) M. M. Davidson, I. H. Hillier, R. J. Hall and N. A. Burton. *J. Am. Chem. Soc.* **116**, 9294 (1994); (c) C. Cativiela, J. I. García, J. A. Mayoral and L. Salvatella. *Chem. Soc. Rev.* **25**, 209 (1996).
19. L. R. Domingo, M. T. Picher, J. Andrés, V. Moliner and V. S. Safont. *Tetrahedron* **52**, 10693 (1996).
20. (a) R. Bonaccorsi, R. Cammi and J. Tomasi. *J. Comput. Chem.* **12**, 301 (1991); (b) I. Tuñón, E. Silla and J. Tomasi. *J. Phys. Chem.* **96**, 9043 (1992).